



Research paper

## Docetaxel-loaded block copolymer micelles labeled with $^{188}\text{Re}$ for combined radiochemotherapy

Elisabete Ribeiro, Fernanda Marques, Lurdes Gano, João D.G. Correia, Isabel Santos, Célia Fernandes\*

*C<sup>2</sup>TN—Center for Nuclear Sciences and Technologies and DECN- Department of Nuclear Engineering and Sciences, Instituto Superior Técnico, Universidade de Lisboa, Portugal*



## ARTICLE INFO

## Keywords:

Cancer  
Chemotherapy  
Docetaxel  
Micelles  
Radionuclide therapy  
Rhenium-188 ( $^{188}\text{Re}$ )

## ABSTRACT

Block copolymer micelles (BCMs), nano-self-assemblies of amphiphilic copolymers with a hydrophobic core surrounded by a hydrophilic corona, were explored for the simultaneous delivery of a lipophilic chemotherapeutic drug and radiation to tumors. Docetaxel (DTX)-functionalized BCMs were radiolabeled with the  $\beta^-$  emitter  $^{188}\text{Re}$  by two different approaches (direct and indirect labelling) affording in both cases  $^{188}\text{Re}$ -Pz-DTX-BCMs with high purity (>98%). The  $^{188}\text{Re}$ -labeled BCMs are stable in PBS pH 7.4 and in cell culture medium, at 37 °C. Cell uptake of  $^{188}\text{Re}$ -Pz-DTX-BCMs in MDA-MB-231 metastatic breast cancer cells and MNNG/HOS osteosarcoma cells presented a maximal uptake of ca. 12% at 24 h incubation time. Biodistribution studies in tumor-bearing nude mice (MDA-MB-231 human xenografts) has shown prolonged circulation lifetime in the bloodstream and moderate uptake in the tumor ( $1.8 \pm 0.8\%$  I.A./g at 24 h *p.i.*). The prolonged blood circulation lifetime together with the *in vivo* stability, suggests that the micelles are potentially useful as drug delivery system to tumors by the EPR effect. As far as we are aware, we describe herein the first example of BCMs,  $^{188}\text{Re}$ -Pz-DTX-BCMs, as versatile nanoplatforams for the simultaneous delivery of beta radiation ( $^{188}\text{Re}$ ) and the chemotherapeutic drug (DTX) potentially useful for cancer therapy. The expected synergistic effect of such combination in pain therapy and/or cancer progression holds promise when compared to the conventional sequential treatment.

## 1. Introduction

Cancer is a major health issue worldwide, being a leading cause of death in countries of all income levels [12,26,28]. It is expected that the number of cancer cases and deaths will grow rapidly in the next years due to several factors [12,26,28]. The most important treatment options available include surgery, radiation therapy and chemotherapy, which is currently supplemented with immunotherapy [19]. Chemotherapy makes use of a great variety of anticancer agents with high efficacy but lacking specificity in the majority of the cases, resulting often in serious toxic effect [22]. Resistance phenomena are also frequently observed for many of these drugs [20]. Moreover, the bioavailability and, consequently, efficacy are quite often affected by intrinsic properties of the drug such as poor water solubility and stability, among others. With the aim of circumventing some of the mentioned drawbacks, sophisticated nanoparticle-based systems are being currently developed for passive or active delivery of anticancer agents to tumor cells [18,21,25]. These

nanoplatforams can also be decorated with targeting moieties and/or imaging units (e.g. fluorescent or radioactive) for image-guided drug delivery [2]. Within this context, we have recently prepared and characterized a novel type of block copolymer micelles (BCMs) containing chelating units on the surface to stabilize the organometallic core *fac*-[M(CO)<sub>3</sub>]<sup>+</sup> for image-guided delivery of therapeutic drugs (M =  $^{99\text{m}}\text{Tc}$ ) or systemic radiotherapy (M =  $^{186/188}\text{Re}$ ) [23]. Additionally, the micelles were loaded with a chemotherapeutic drug, docetaxel (DTX) used in the treatment of various cancers (e.g., breast cancer, prostate cancer or non-small cell lung cancer) whose release from the nanoparticle was favored by low pH. It has been also demonstrated that the anti-proliferative activity of the DTX-loaded micelles is significantly higher than that of free DTX for the same concentration in various cancer cell lines. This indicated that a similar therapeutic outcome may be potentially achieved with reduced side effects. Moreover, the  $^{99\text{m}}\text{Tc}$ -labeled micelles are taken up by those cells, being in agreement with the anti-proliferative activity observed. Preliminary biodistribution

\* Corresponding author. *C<sup>2</sup>TN—Centro de Ciências e Tecnologias Nucleares, Instituto Superior Técnico, Universidade de Lisboa, Estrada Nacional 10, (km 139,7), 2695-066, Bobadela LRS, Portugal.*

*E-mail address:* [celiaf@ctn.tecnico.ulisboa.pt](mailto:celiaf@ctn.tecnico.ulisboa.pt) (C. Fernandes).

<https://doi.org/10.1016/j.jddst.2020.101898>

Received 24 May 2020; Accepted 27 June 2020

Available online 17 July 2020

1773-2247/© 2020 Elsevier B.V. All rights reserved.

studies in healthy mice have shown relevant *in vivo* stability and adequate pharmacokinetic profile. Brought together, these results prompted us to explore these micelles for the simultaneous delivery of an anticancer agent such as DTX and  $^{188}\text{Re}$ , a  $\beta^-$ -emitting radionuclide considered a “theranostic pair” of  $^{99\text{m}}\text{Tc}$ . Rhenium-188 has a physical half-life of 16.9 h, with a  $\beta^-$  average energy emission of 784 keV and a maximum energy of 2.12 MeV, sufficient to penetrate and destroy targeted abnormal tissues [8,17]. Additionally, has also a gamma emission of 155 keV (15%) useful for imaging and for dosimetric estimation. Furthermore, the availability of  $^{188}\text{Re}$  from the  $^{188}\text{W}/^{188}\text{Re}$  generator system is an important feature and permits installation in hospital-based or central radiopharmacies for cost-effective availability of no-carrier-added (NCA)  $^{188}\text{Re}$  [8,17]. In addition, the combination of chemotherapeutic drugs with ionizing radiation (chemoradiotherapy), either externally (from an external beam) or internally (e.g., targeted radionuclide therapy), is an established therapeutic procedure [9,24].

Targeted radionuclide therapy in combined-modality therapeutic regimens is emerging as a potent tool for destroying malignant cells while sparing healthy tissues [9]. Taxanes in particular, namely DTX or Paclitaxel, have been studied in combination with ionizing radiation in animal models, and a significant supra-additive response has been observed [3].

As regards the combination of Re radioisotopes with docetaxel in Phase I/II clinical trials have shown that  $^{186/188}\text{Re}$ -hydroxyethylidene diphosphonate (HEDP) in metastatic castrate-resistant prostate cancer can be safely combined with docetaxel, and a survival benefit was observed for  $^{188}\text{Re}$ -HEDP [4,5].

Aiming to assess the pharmacological advantages of combining  $^{188}\text{Re}$  with DTX in the same multifunctional nanoplatform, compared to the “conventional” sequential treatments, herein, we describe the preparation, characterization and biological evaluation of DTX-loaded  $^{188}\text{Re}$ -labeled multifunctional block copolymer micelles. This type of platforms may allow exploitation of synergistic interactions between ionizing radiation and chemotherapy.

## 2. Experimental procedure

### 2.1. Materials

All chemicals and solvents were of reagent grade and used without further purification unless otherwise stated. Docetaxel anhydrous (DTX) was purchased from Chemos GmbH. The copolymers Me-PEG-b-PCL and Pz-PEG-b-PCL were prepared as previously described [23]. Poly(ethylene glycol) methyl ether (Me-PEG,  $M_n = 5000$ ), from Sigma-Aldrich, and O-(2-Aminoethyl)polyethylene glycol ( $\text{NH}_2$ -PEG,  $M_n = 3000$ ), from Fluka, were dried twice by azeotropic distillation in toluene that was distilled off completely. Sigma-Aldrich  $\epsilon$ -caprolactone (CL) was dried using calcium hydride and distilled prior to use.

Carrier-free  $\text{Na}[^{188}\text{ReO}_4]$  was freshly eluted from a commercial  $^{188}\text{W}/^{188}\text{Re}$  generator (ITG), using 0.9% saline solution. The radiochemical purity of  $\text{Na}[^{188}\text{ReO}_4]$  was higher than 95% as determined by ITLC-SG (Glass Microfibre Chromatography Paper impregnated with silica gel) using saline solution as eluent. The radionuclide purity of  $^{188}\text{Re}$  was analyzed by gamma spectroscopy with a high-purity germanium (HPGe) detector.

### 2.2. Methods

HPLC analysis was performed on a Perkin-Elmer LC pump 200 coupled to a LC tunable UV-VIS detector (227 nm). The solvents were of HPLC grade. DTX analysis was performed in a EC 250/4 mm (L/ID) Nucleosil 100-10 C18 column using an isocratic method with a flow rate of 1 mL/min for 15 min and acetonitrile and trifluoroacetic acid (TFA) 0.1% aqueous (50/50, v/v) as the mobile phase. DTX was quantified with reference to a calibration curve.

The radiolabeled copolymers and micelles were analyzed by ITLC-SG

using as mobile phase methanol/12 N HCl (99/1, v/v) or saline, respectively.

### 2.3. Preparation and characterization of copolymers and micelles

The copolymers methoxy-terminated poly(ethylene glycol)-b-poly( $\epsilon$ -caprolactone) (Me-PEG-b-PCL), amino-terminated poly(ethylene glycol)-b-poly( $\epsilon$ -caprolactone) ( $\text{NH}_2$ -PEG-b-PCL) were synthesized by metal-free cationic ring-opening polymerization of  $\epsilon$ -caprolactone ( $\epsilon$ -CL) via an activated monomer mechanism with HCl-diethyl ether and characterized, following reported synthetic methodologies [29]; Liu et al., 2007). Also, the block copolymer pyrazolyl-diamine poly(ethylene glycol)-b-poly( $\epsilon$ -caprolactone) (Pz-PEG-b-PCL) was synthesized and characterized as published previously [23].

DTX encapsulated BCMS (DTX-BCMS) were prepared by the thin-film hydration method [11]. Briefly, 50 mg of MePEG-b-PCL copolymer and 2.3 mg of DTX were dissolved in DMF. After 4 h with continuous stirring was dried under nitrogen to form a DTX/copolymer film, and subsequently hydrated with 0.01 M phosphate buffer pH 7.4 at 60 °C to form DTX-BCMS. The new block copolymer Pz-PEG-b-PCL was incorporated into DTX loaded BCMS by transfer method forming functionalized loaded micelles, Pz-DTX-BCM: Briefly, 400  $\mu\text{L}$  of Pz-PEG-b-PCL ( $1.25 \times 10^{-4}$  M) in PB was added to 2 mg of DTX-BCMS dissolved in 2 mL of PB at 60 °C, also in PB. The mixture was maintained under stirring for 1 h at 60 °C and overnight at RT and then lyophilized.

Before using, all the micelles were dissolved in 0.01 M phosphate buffer, pH 7.4 (PB) in order to obtain 1 g/L solutions that were subsequently sonicated for 20 min.

For determination of shape and morphology, micelles were dissolved in 0.01 M PB, pH 7.4 at 0.1 g/L and were placed on negatively charged carbon-coated copper grids and left to dry at RT and were observed by transmission electron microscopy (TEM) with a Hitachi H-8100 electron microscope operating at 500 keV. Also, micelle surface area was calculated by IMAGEJ image processing software. To hydrodynamic diameter ( $D_h$ ), and zeta potential determination, using a Zetasizer Nano ZS from Malvern with zeta-potential cells, the micelles solutions (1 g/L, in 0.01 M PB pH 7.4) were diluted 10x and filtered using a 0.20  $\mu\text{m}$  syringe filter. The particle size was measured by dynamic light scattering (DLS) at 25 °C with a 173° scattering angle, and an optic arrangement known as non-invasive back scatter (NIBS).

The DTX loading content (LC) was determined by RP-HPLC with reference to a standard calibration curve. Briefly, 4 mg of loaded BCMS were dissolved in 500  $\mu\text{L}$  of acetonitrile, sonicated and centrifuged at 3000 g for 10 min to precipitate the copolymer. The supernatant was collect and analyzed by HPLC as describe above. The LC was calculated by the ratio of entrapped DTX over the total amount of micelles.

### 2.4. Preparation of $[\text{}^{188}\text{Re}(\text{CO})_3(\text{H}_2\text{O})_3]^+$

The radioactive precursor *fac*- $[\text{}^{188}\text{Re}(\text{CO})_3(\text{H}_2\text{O})_3]^+$  was prepared as described in the literature [7]. Briefly, 1.0 mL (267.5–696.7 MBq) of carrier-free  $\text{Na}[^{188}\text{ReO}_4]$  mixed with 4  $\mu\text{L}$  of  $\text{H}_3\text{PO}_4$  (85%) was added to a vial containing 5 mg of  $\text{BH}_3\cdot\text{NH}_3$  and 3 mg of  $\text{K}_2[\text{H}_3\text{BCO}_2]$ , flushed with nitrogen, and incubated at 60–75 °C for 15–20 min. In order to keep the balance of  $\text{H}_2$  gas formed during the reaction, a 20 mL syringe was used.

### 2.5. Micelles labeling with $[\text{}^{188}\text{Re}(\text{CO})_3(\text{H}_2\text{O})_3]^+$

DTX encapsulated BCMS (DTX-BCMS) were prepared by the thin-film hydration method and used to prepare the functionalized micelles (Pz-DTX-BCMS) by the transfer method as previously described [23]. Before using, all the micelles were dissolved in 0.01 M phosphate buffer, pH 7.4 (PB) in order to obtain 1 g/L solutions that were subsequently sonicated for 20 min.

The radiolabeled micelles were obtained using two different

methods: direct and indirect labelling (Fig. 1).

### 2.5.1. Direct labeling procedure

To a nitrogen-purged glass vial containing 1.0 mg of functionalized micelles (Pz-DTX-BCMs), was added 1.0 mL (65.1–68.1 MBq) of  $fac-[^{188}\text{Re}(\text{CO})_3(\text{H}_2\text{O})_3]^+$ . The reaction mixture was incubated at 60 °C for 90 min and, after cooling, the radiolabeled micelles were purified by 10 kDa Amicon centrifugal filters. The radiochemical yield and purity were assessed by ITLC-SG using saline as eluent.

### 2.5.2. Indirect labeling procedure

A glass vial containing 0.14 mg of the copolymer Pz-PEG-*b*-PCL was flushed with nitrogen and 1.0 mL (44.4–65.1 MBq) of  $fac-[^{188}\text{Re}(\text{CO})_3(\text{H}_2\text{O})_3]^+$  was added. The vial was incubated at 60 °C for 60 min to obtain the radiolabeled copolymer that was purified using 10 kDa Amicon centrifugal filters. The radiolabeled copolymer was incorporated into the loaded DTX-BCMs by the transfer method: For this, the labeled copolymer  $^{188}\text{Re}(\text{I})$ -Pz-PEG-*b*-PCL was added to a vial containing 1.1 mg of DTX-loaded micelles (DTX-BCMs) dissolved in 200  $\mu\text{L}$  of 0.01 M phosphate buffer, pH7.4 (PB). The reaction mixture was left under stirring for 1 h at 60 °C followed by incubation overnight at room temperature. Then, the radiolabeled BCMs ( $^{188}\text{Re}$ -Pz-DTX-BCMs) were purified and concentrated also using the Amicon centrifugal filters.

The radiochemical labeling yield as well as the radiochemical purity of the labeled copolymer and micelles were determined by ITLC-SG using the eluent described above.

### 2.6. In vitro stability studies

The *in vitro* stability of  $^{188}\text{Re}$  labeled micelles and copolymer was evaluated at 37 °C in PBS (pH 7.4, 0.01 M) and in cell culture medium (Dulbecco's modified Eagle's medium, DMEM) by ITLC-SG/saline at different time points (4 h, 24 h).

### 2.7. Cellular uptake

The cellular uptake experiments were performed in human tumor cell lines, namely MDA-MB-231 breast adenocarcinoma and MNNG/HOS osteosarcoma cell lines (ATCC). The cells were cultured in DMEM

(Dulbecco's Modified Eagle Medium) with GlutaMAX™ (Gibco) supplemented with 10% fetal bovine serum in culture flasks until confluence. For the assays, cells were trypsinized with trypsin-EDTA and seeded at a density of  $2.5 \times 10^5$  cells/500  $\mu\text{L}$  in 24-well plates. Cells were allowed to adhere for 24 h and then were incubated with  $\sim 37$  kBq/0.5 mL ( $\sim 1$   $\mu\text{Ci}$ /0.5 mL) of the radiolabeled BCMs in media at 37 °C for different time points (1 h – 24 h). Incubation was ended by washing the cells with ice-cold medium followed by a two wash steps with cold PBS. After the washing steps, the cells were lysed by 15 min incubation with 1 M NaOH at 37 °C to assess the cellular associated radioactivity. Wells without cells were used to check the unspecific binding of the radiolabeled BCMs, following a similar procedure as described above. Up to 24 h the radioactivity present in the NaOH lysing solution was negligible, of the same order as the radiation background. The radioactivity in the media and in the cells were separated, collected and counted in a  $\gamma$  counter. Cellular uptake data was based on three determinations for each time point and are expressed as mean  $\pm$  SD.

### 2.8. Animal studies

All mice were housed at C<sup>2</sup>TN-IST animal facilities and maintained in pathogen-free ventilated cages under controlled conditions of temperature and humidity with 12 h light/12 h dark schedule and free access to standard diet and water *ad libitum*.

#### 2.8.1. Ethical statement

Animal studies were carried out under the supervision of well-experienced researchers in laboratory animal facilities licensed by the National Authority in compliance with the principles of laboratory animal science on animal care, protection and welfare and are properly accredited by the respective National Authorities according to the national (DL 113/2013) and EU (Directive 63/2010/EU) legislation. The research project was also approved by the National Authority.

#### 2.8.2. Biodistribution

The biodistribution profile of the  $^{188}\text{Re}$ -Pz(DTX)BCMs was evaluated in separated groups of Nude CBA mice weighting between 16 and 25 g each with and without MDA-MB-231 xenograft.

**MDA-MB-231 xenografts** -The mouse breast carcinoma xenograft model was established by injecting subcutaneously  $5 \times 10^6$  viable MDA-MB-231 cells (in 0.15 mL fresh culture medium:Matrigel suspension, 1:1) into the right flank of each mouse. Animals were monitored daily for tumor size, general physical conditions and body weight. Ten to twelve days later mice developed well-palpable tumors.

For biodistribution evaluation separated groups of both animal models were intravenously injected with 100  $\mu\text{L}$  (8.5–16.0 MBq) of each preparation via the tail vein and were maintained on normal diet *ad libitum*. At 4 h and 24 h post-injection (*p.i.*) mice were sacrificed by cervical dislocation. The radioactive administered dose and the radioactivity in the sacrificed animal were measured in a dose calibrator (Capintec CRC25R). The difference between the radioactivity in the injected and sacrificed animal was assumed to be due to excretion. Blood samples were taken by cardiac puncture at sacrifice. Tissue samples of the main organs were then removed, weighted and counted in a gamma counter (LB2111, Berthold, Germany). The uptake in the organs/tissues was calculated and expressed as a percentage of the injected activity per gram (%I.A./g).

#### 2.8.3. In vivo stability

The stability of the radiolabeled micelles was assessed in urine and murine blood serum by ITLC-SG analysis under the analytical conditions described above to check the radiochemical purity of the radiolabeled micelles. The samples were taken at the sacrifice time 24 h post injection. The urine collected was filtered through a Millex GV filter (0.22  $\mu\text{m}$ ) before ITLC-SG analysis. Blood collected from the mice was centrifuged at 3000 rpm for 15 min and the serum was separated and

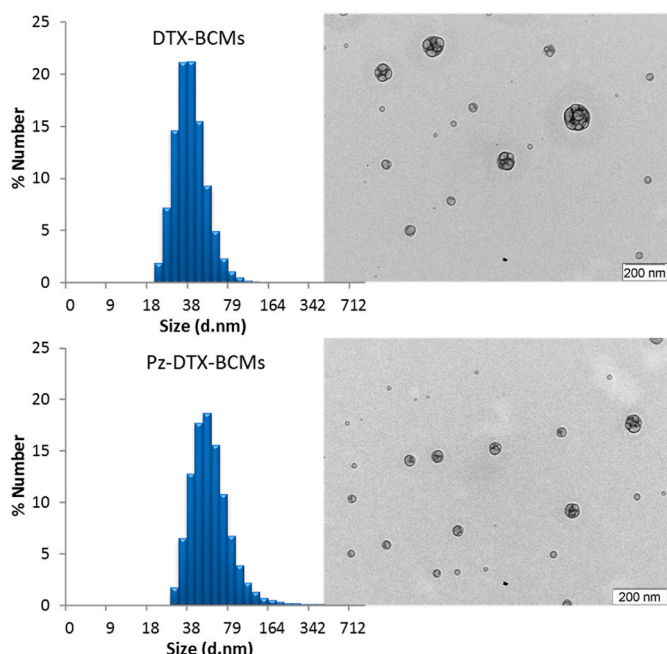


Fig. 1. DLS histogram and TEM image of DTX-BCMs and Pz-DTX-BCMs.

analyzed by ITLC-SG/saline.

### 2.9. Statistical analysis

Values are expressed as means and the error bars in graphs represent the standard error of the means (SEM). All statistical comparisons were done with the GraphPad Prism 6.0 software for Windows (GraphPad software). Multiple comparison of means was done with the one-way ANOVA test, using Dunnett's multiple comparison test. To exclude experimental outliers, Grubbs' test was used. The level of statistical significance was set at  $p < 0.05$ . \* $p < 0.05$ , \*\* $p < 0.01$ , \*\*\* $p < 0.001$  and \*\*\*\* $p < 0.0001$ .

## 3. Results and discussion

The copolymers Me-PEG-*b*-PCL, NH<sub>2</sub>-PEG-*b*-PCL and Pz-PEG-*b*-PCL were synthesized by metal-free cationic ring-opening polymerization of  $\epsilon$ -caprolactone (CL) and characterized by <sup>1</sup>H NMR and FTIR spectroscopy as described by us [23]. The molecular weight and chemical composition of the copolymers were determined based on the known molecular weight of the PEG precursors and the intensity ratio of the methylenic peak of the PEG block (at  $\delta$  4.20) and the resonance of the PCL block (at  $\delta$  2.28) at <sup>1</sup>H NMR spectra. Taking the calculated number of CL monomers, which was similar (ca. 45) for Me-PEG-*b*-PCL and NH<sub>2</sub>-PEG-*b*-PCL, the estimated molecular weight for Me-PEG-*b*-PCL, NH<sub>2</sub>-PEG-*b*-PCL and Pz-PEG-*b*-PCL was 10000 Da, 8000 Da and 8400 Da, respectively.

The pyrazolyl-diamine chelating unit (Pz) with a *N,N,N*-donor atom set was selected as it gives M(CO)<sub>3</sub> (M = <sup>99m</sup>Tc, <sup>188</sup>Re), radiometallated complexes with high *in vitro* and *in vivo* stability even for <sup>188</sup>Re [7].

### 3.1. Preparation and characterization of micelles

The DTX-loaded micelles (DTX-BCMs) and DTX-loaded BCMs functionalized with a pyrazolyl-diamine chelating unit (Pz-DTX-BCMs; Pz = pyrazolyl-diamine chelating unit) on the surface were prepared following a previously reported procedure [23]. Briefly, DTX-BCMs, were prepared using the thin-film hydration method and the copolymer Pz-PEG-*b*-PCL was introduced by the transfer method to afford the functionalized micelles Pz-DTX-BCMs [10,11,23,29]. The micelles (DTX-BCMs and Pz-DTX-BCMs) were characterized by transmission electron microscopy (TEM) and dynamic light scattering (DLS) and their main properties are summarized in Table 1.

The morphology of the BCMs was evaluated by TEM and revealed a spherical morphology and a relatively uniform size distribution (Fig. 1). Through the IMAGEJ image processing software, the micelle surface area was calculated and used to determine the diameter of the micelles: 30.5 ± 8.0 nm and 42.8 ± 15.6 nm to DTX-BCMs and Pz-DTX-BCMs, respectively. These values were similar to the ones obtained for the relative hydrodynamic diameter (D<sub>h</sub>) which were determined by dynamic light scattering (DLS): 39.0 ± 4.6 nm and 58.6 ± 7.8 nm to DTX-BCMs and Pz-DTX-BCMs, respectively (Table 1, Fig. 1).

The measured zeta-potentials, -1.8 ± 1.2 mV and -4.5 ± 2.3 mV, for

**Table 1**  
Hydrodynamic diameter (D<sub>h</sub>), Zeta Potential and DTX Loading Content (LC) of Micelles [23].

.Micelles	Size (nm)		PDI	Zeta <sup>a</sup> potential (mV)	LC(%)
	TEM <sup>a</sup>	D <sub>h</sub> <sup>b</sup>			
DTX-BCMs	30.5 ± 8.0	39.0 ± 4.6	0.42 ± 0.01	-1.8 ± 1.2	3.2 ± 0.3
	42.8 ± 15.6	58.6 ± 7.8	0.36 ± 0.01		
Pz-DTX-BCMs	42.8 ± 15.6	58.6 ± 7.8	0.36 ± 0.01	-4.5 ± 2.3	0.55 ± 0.05
	15.6	7.8	0.01		

<sup>a</sup> Micelle surface area was calculated by IMAGEJ image processing software.

<sup>b</sup> Mean ± SD of distribution by number (refractive index = 1.5).

DTX-BCMs and Pz-DTX-BCMs respectively, are very promising since they indicate low serum protein aggregation and reduced mononuclear phagocyte system (MPS) uptake important parameters for passive targeting [6,10,27].

A key parameter in micelle formation and thermodynamic stability is the critical micelle concentration (CMC) defined as the minimal concentration at which amphiphilic copolymer chains are thermodynamically driven to self-assemble in aqueous solution forming micelles. The CMC was determined by a fluorescence-based method using pyrene as fluorescent probe [23]. A CMC of 4 mg/L is described for the copolymer Me-PEG-*b*-PCL while for the copolymer Pz-PEG-*b*-PCL the reported CMC is 65 mg/L. Usually, micelles that are formed at low CMC are more stable *in vivo*, even after diluted in the bloodstream [1,16].

The DTX loading content (LC) is the ratio of the entrapped DTX in the micelles over the total amount of loaded micelles and it was determined by HPLC with reference to a standard calibration curve as described in the experimental section [11]. With the addition of the new functionalized copolymer the LC decreased from 3.2 ± 0.3% to 0.55 ± 0.05% (Table 1) due to the addition of a new copolymer.

### 3.2. Preparation of <sup>188</sup>Re-Pz-DTX-BCMs

The radiolabeling of the multifunctional BCMs with <sup>188</sup>Re was accomplished by reaction of the organometallic precursor *fac*-[<sup>188</sup>Re(CO)<sub>3</sub>(H<sub>2</sub>O)<sub>3</sub>]<sup>+</sup> with the pyrazolyl-diamine ligand present in the copolymer. The organometallic precursor *fac*-[<sup>188</sup>Re(CO)<sub>3</sub>(H<sub>2</sub>O)<sub>3</sub>]<sup>+</sup> was prepared by direct reduction of sodium perrhenate ([<sup>188</sup>ReO<sub>4</sub>]<sup>-</sup>), eluted from a <sup>188</sup>W/<sup>188</sup>Re generator (ITG) using a reported procedure [7].

Taking into consideration the half-life of the radionuclide <sup>188</sup>Re (t<sub>1/2</sub> = 17 h) two different approaches for the synthesis of <sup>188</sup>Re-Pz-DTX-BCMs were considered, namely the i) direct labelling and ii) indirect labelling approaches (Fig. 2).

#### i) Direct labeling – Labeling of preformed micelles

The radiolabeled micelles <sup>188</sup>Re-Pz-DTX-BCMs were obtained by reaction of the organometallic precursor *fac*-[<sup>188</sup>Re(CO)<sub>3</sub>(H<sub>2</sub>O)<sub>3</sub>]<sup>+</sup> with the functionalized micelles (Pz-DTX-BCMs) following the same procedure previously described by us for the radiolabeling of this micelles with <sup>99m</sup>Tc [23]. Unlike the good radiolabeling yield (82%) achieved with <sup>99m</sup>Tc, the <sup>188</sup>Re-Pz-DTX-BCMs were obtained with low radiolabeling yield (approximately 21%) using the same experimental conditions. Consequently, a thorough optimization of the radiolabeling procedure was undertaken. Labeling parameters such as temperature, incubation time, amount of BCMs, type of solvent and dissolution conditions (use of ultrasound) were studied. Despite our efforts, the radiolabeling yield remained relatively low (approximately 30%). Nevertheless, <sup>188</sup>Re-Pz-DTX-BCMs were easily purified by ultrafiltration (10 kDa Amicon centrifugal filters) and were obtained with high purity (>98%).

#### ii) Indirect labelling

Considering both the low radiolabeling yield obtained by the direct labelling approach and the relatively long half-life of <sup>188</sup>Re we have evaluated the possibility of preparing <sup>188</sup>Re-Pz-DTX-BCMs through an indirect labelling approach like the one used by Hoang [11]. In this case, the functionalized copolymer (Pz-PEG-*b*-PCL) firstly reacts with the precursor *fac*-[<sup>188</sup>Re(CO)<sub>3</sub>(H<sub>2</sub>O)<sub>3</sub>]<sup>+</sup> affording the radiolabeled copolymer <sup>188</sup>Re-Pz-PEG-*b*-PCL that, after purification, could be incorporated into the DTX-BCMs by the transfer method giving the radiolabeled micelles. In this way, we expected higher labelling yields since the concentration of Pz-PEG-*b*-PCL in the labelling mixture can be increased and more efficient labelling conditions (e.g. higher temperature) could be used because the sensitive BCMs were not yet formed. The main drawback of such strategy is the longer time to perform the overall radiolabelling procedure. In brief, the copolymer Pz-PEG-*b*-PCL reacted with

## i) Direct labelling

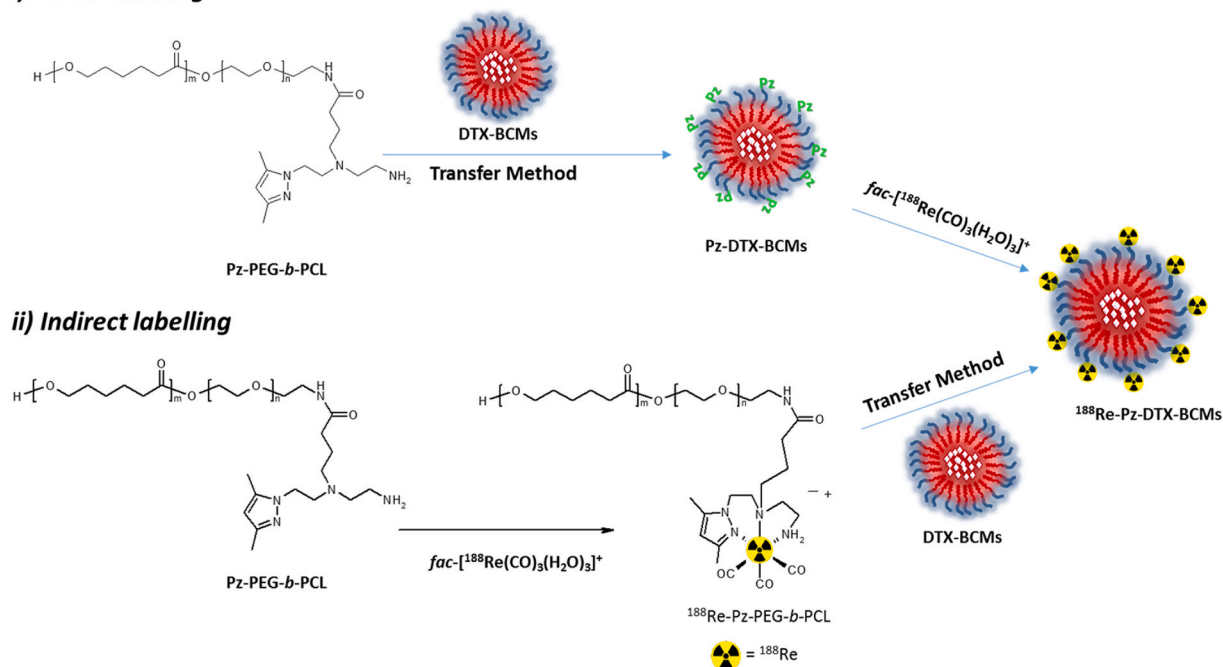


Fig. 2. Synthesis of  $^{188}\text{Re}$ -Pz-DTX-BCMs by the i) direct and ii) indirect labelling approaches.

$\text{fac-}[^{188}\text{Re}(\text{CO})_3(\text{H}_2\text{O})_3]^+$  (60 min, 60 °C) to afford the radiolabeled copolymer  $^{188}\text{Re}$ -Pz-PEG-*b*-PCL ( $\eta = 80\%$ ), which was used to prepare the radiolabeled BCMs by the transfer method. The overall radiolabeling yield was much higher, when compared to the direct method described above. Nevertheless, in both methods, the radiolabeled micelles were obtained with high purity (>98%) after purification by ultrafiltration.

3.3. *In vitro* stability studies

One of the main problems associated with the use of radioactive rhenium compounds for systemic radiotherapy is related with their higher tendency to re-oxidize to perrhenate ([e.g.  $^{188}\text{ReO}_4^-$ ]) in comparison with the  $^{99\text{m}}\text{Tc}$  analogs. In fact, in the preparation of  $^{188}\text{Re}$ -HEDP the bone fixation is strongly dependent of *in vivo* stability [13,14,17]. Several authors have studied the influence of the reaction

conditions and kit composition on  $^{188}\text{Re}$ -HEDP stability and *in vivo* behavior [13,14]. All of them pointed out that the addition of carrier was decisive to achieve good *in vivo* stability and high bone uptake. In the case of the  $^{188}\text{Re}$ -labeled micelles, it is important to avoid the reoxidation of the radiometal and the integrity and intrinsic properties of the micelles must be preserved keeping their ability to deliver radiation and/or encapsulated drugs to the tumor by the enhanced permeability and retention (EPR) effect. Therefore, we have evaluated the *in vitro* stability of the  $^{188}\text{Re}$ -DTX-BCMs (prepared by the direct and indirect method) upon incubation in phosphate-buffered saline (PBS) pH 7.4 and in cell culture media DMEM (Dulbecco's Modified Eagle Medium) at 37 °C up to 24 h. Samples collected at various time points were analyzed by the chromatographic system ITLC-SG/saline (Fig. 3). The results have shown that the radiolabeled BCMs were stable *in vitro* independently of the incubation media or the radiolabeling method used for their

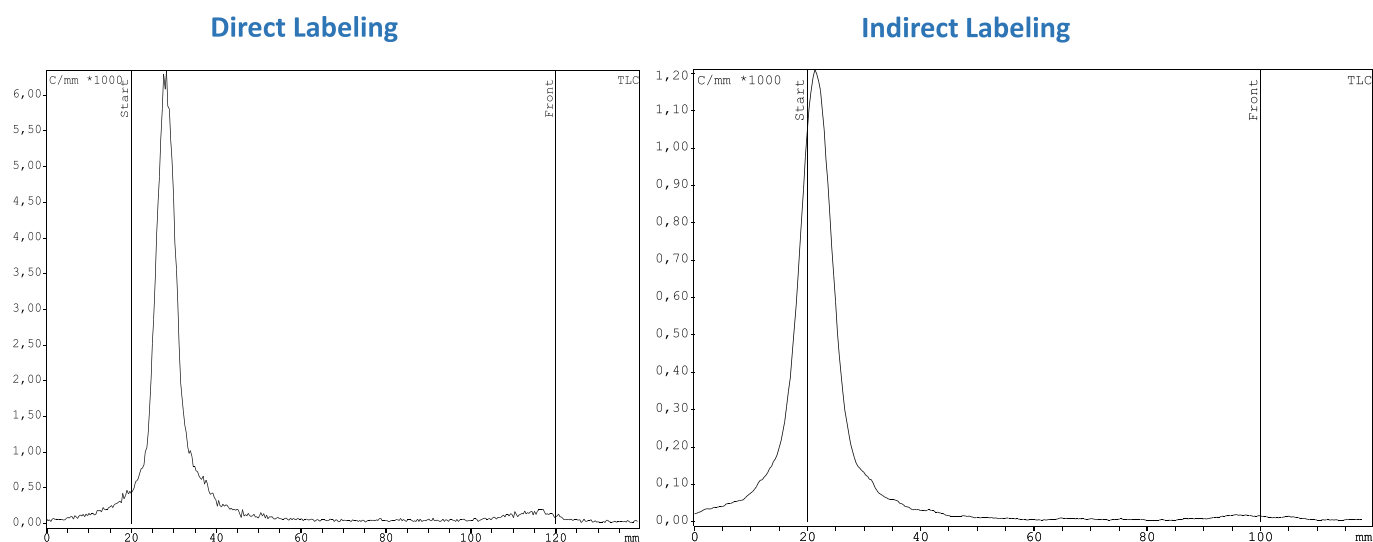


Fig. 3. Radiochromatograms of  $^{188}\text{Re}$ -Pz-DTX-BCMs obtained by direct (left) and indirect (right) method, incubated 24 h in PBS pH 7.4, at 37 °C. Chromatographic system: ITLC-SG/Saline; In this chromatographic system  $^{188}\text{Re}$ -Pz-DTX-BCMs stay at origin ( $R_f = 0-0.1$ ).

preparation.

### 3.4. Cell studies

The cellular uptake of  $^{188}\text{Re}$ -Pz-DTX-BCMs in the MDA-MB-231 breast cancer and MNNG/HOS osteosarcoma cell lines was assessed at different time points up to 24 h (Fig. 4). Both cell lines showed a similar uptake trend, i.e., a fast increase until 3 h incubation time followed by a relatively slow increase up to 17 h and a steady phase between 17 h and 24 h. Maximum uptake in both cell lines was similar (~12%). Interestingly, a quite similar uptake behavior was also observed for the  $^{99\text{m}}\text{Tc}$ -labeled BCMs previously described, using the same cell lines [23].

### 3.5. Animal studies

As mentioned before, a major concern associated with the use of  $^{188}\text{Re}$ -labeled molecules or nanoparticles is the *in vivo* stability and the eventual reoxidation to  $^{188}\text{ReO}_4^-$ , which might impair their utility for target specific systemic radiotherapy. Thus, aiming to assess the *in vivo* stability of the radiolabeled micelles and respective biodistribution profile a preliminary biodistribution study with  $^{188}\text{Re}$ -Pz-DTX-BCMs, obtained either by the direct or indirect method, was carried out in healthy immunodeficient Nude CBA mice at 4 h and 24 h post intravenous injection (p.i.).

The stability of the radiolabeled micelles was assessed by radiochromatographic analysis of urine and serum samples collected at sacrifice under the experimental conditions described above for the radiolabeled micelles.

Interestingly, the results have clearly demonstrated that the radiolabeling methodology used to prepare the  $^{188}\text{Re}$ -labeled BCMs plays a crucial role in their *in vivo* stability in contrast with their *in vitro* stability discussed above. In fact, only the  $^{188}\text{Re}$ -labeled BCMs obtained by the direct radiolabeling approach are stable *in vivo* 24 h p.i., as shown in Fig. 5. Consequently, further biodistribution studies were performed using only the radiolabeled micelles obtained by the direct radiolabeling method.

Further preliminary biodistribution studies of  $^{188}\text{Re}$ -Pz-DTX-BCMs were carried out in normal nude CBA mice and in MDA-MB-231 human breast cancer xenografted CBA mice after intravenous administration. In

this way, it will be possible to get an insight into the tissue distribution profile and ability to accumulate in tumors. Results of these studies are summarized for the most relevant organs and tumor in Figs. 6 and 7. The uptake in the tissues was calculated and expressed as a percentage of the injected activity per gram of tissue (% I.A./g  $\pm$  SD). The whole-body radioactivity excretion was determined as a percentage of the total injected activity. The main features of the *in vivo* behaviour of  $^{188}\text{Re}$ -Pz-DTX-BCMs are the relatively slow clearance from blood ( $11.2 \pm 0.9$  and  $4.6 \pm 1.5\%$  I.A./g blood at 4 h and 24 h p.i., respectively) via both the hepatic and the renal pathways. Consequently, some radioactivity accumulation was detected in highly irrigated organs such as lungs and heart due to the radioactivity accumulation in the blood compartment. The low uptake in the stomach indicate that no significant reoxidation to  $^{188}\text{ReO}_4^-$ , happened *in vivo*. High hepatic uptake was found at 4 h p.i. ( $12.1 \pm 0.2\%$  I.A./g) that decreased at 24 h p.i. ( $5.2 \pm 0.5\%$  I.A./g) indicating the involvement of hepatobiliary excretory pathway. Besides this pathway, a renal elimination mechanism was also involved, since relevant kidney uptake was found ( $6.9 \pm 0.2\%$  I.A./g at 4 h p.i.) that was mostly retained at 24 h ( $4.8 \pm 0.9\%$  I.A./g). The overall rate of radioactivity excretion was moderate (<50%) at 24 h p.i.

$^{188}\text{Re}$ -Pz-DTX-BCMs were predominately taken by the spleen ( $41.5 \pm 6.8\%$  I.A./g, at 4 h p.i.) decreasing its accumulation at 24 h p.i. ( $26.9 \pm 4.5\%$  I.A./g). This finding is not in accordance with the biodistribution profile found for the  $^{99\text{m}}\text{Tc}$ -labeled micelles, which presented a moderate spleen uptake [23]. However, high splenic uptake in addition with the liver uptake is a common distribution profile in micelle formulations [10,15]. In general, they are mostly taken and cleared by the mononuclear phagocyte system organs showing high uptake in the liver and spleen [6,10,15,27].

A similar distribution pattern was found for the tumor-bearing animal model as evidenced in Fig. 5. A slow blood clearance with predominant hepatic and splenic uptake with some radioactivity excretion via the urinary path was found. The overall rate of radioactivity excretion was  $58.4 \pm 7.0\%$  I.A.

Regarding the ability to target the MDA-MB-231 human xenografts,  $^{188}\text{Re}$ -Pz-DTX-BCMs were taken by the tumors ( $1.8 \pm 0.8\%$  I.A./g at 24 h p.i.) but the tumor-to-blood radioactivity ratio was quite disappointing ( $0.5 \pm 0.1$ ) at this time point which may suggest that the incorporation of a tumor-targeting specific unit on the micelles would potentially improve its drug delivery efficacy.

## 4. Conclusions

DTX-loaded BCMs were successfully radiolabeled with the organometallic synthon  $\text{fac-}^{188}\text{Re}(\text{CO})_3^+$  using two different strategies affording  $^{188}\text{Re}$ -Pz-DTX-BCMs with high purity. The stability of the  $^{188}\text{Re}$ -labeled micelles is dependent on the labelling strategy since only those obtained by the direct labeling approach presented high *in vivo* stability. Biodistribution studies in tumor-bearing mice has shown prolonged circulation lifetime in the bloodstream and moderate uptake in the tumor. Brought together the biodistribution studies, namely the combination of prolonged blood circulation lifetime and *in vivo* stability, suggest that the micelles are potentially useful as drug delivery system to tumors by the EPR effect. Incorporation of a tumor-targeting unit on the micelles would potentially improve drug delivery and therapeutic efficacy. A synergistic effect could be also explored between the chemotherapy agent, DTX, and the  $\beta^-$  particles (radiotherapy). Moreover,  $^{188}\text{Re}$  is also a  $\gamma$  emitter (155 KeV, 15%) allowing SPECT-imaging to be used for dosimetry purposes, biodistribution and following therapeutic efficacy. In conclusion, to the best of our knowledge we describe herein the first example of BCMs,  $^{188}\text{Re}$ -Pz-DTX-BCMs, as versatile nanoplat-forms for the simultaneous delivery of beta radiation ( $^{188}\text{Re}$ ) and a chemotherapeutic drug (DTX) potentially useful for cancer therapy. The synergistic effect of such combination, in pain therapy and/or cancer progression, would be beneficial when compared to the conventional sequential treatment.

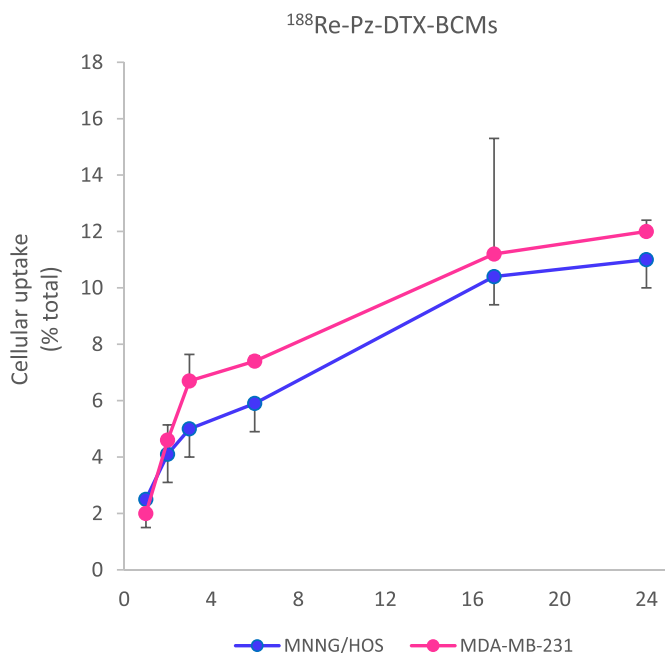


Fig. 4. Cellular uptake profile of  $^{188}\text{Re}$ -Pz-DTX-BCMs in MDA-MB-231 and MNNG/HOS cells with time of incubation.

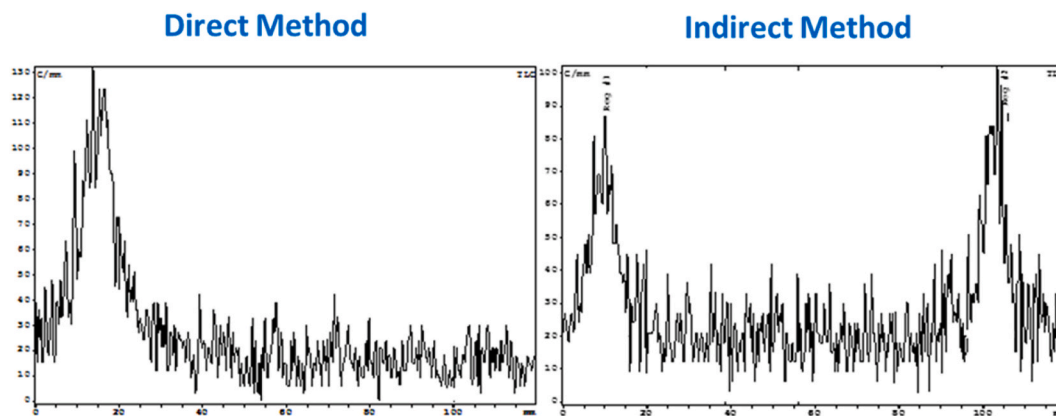


Fig. 5. Blood serum analysis (ITLC-SG/Saline) of  $^{188}\text{Re}$ -Pz-DTX-BCMs obtained by direct (left) and indirect (right) method, 24 h p.i. in nude CBA mice. In this chromatographic system  $^{188}\text{Re}$ -Pz-DTX-BCMs stay at origin ( $R_f = 0-0.1$ ).

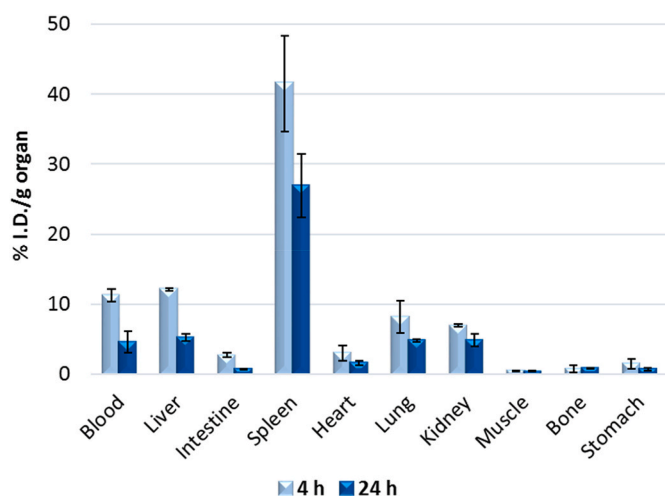


Fig. 6. Biodistribution of  $^{188}\text{Re}$ -Pz-DTX-BCMs in nude CBA mice at 4 h and 24 h p.i., expressed as %I.A./g.

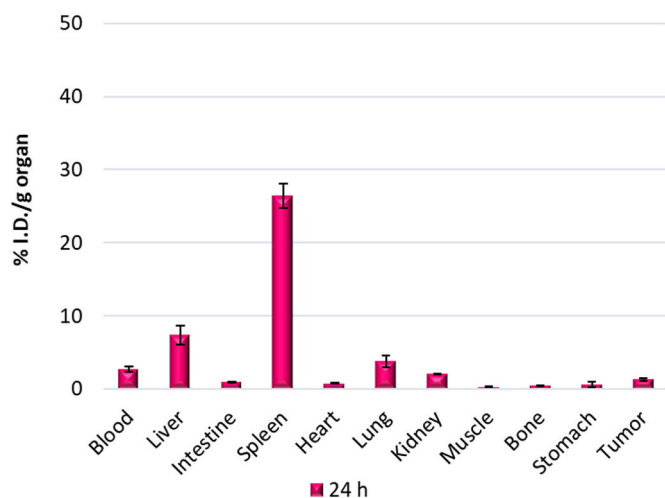


Fig. 7. Biodistribution of  $^{188}\text{Re}$ -Pz-DTX-BCMs in MDA-MB-231 xenografted nude CBA mice at 24 h p.i., expressed as %I.A./g.

## Acknowledgements

This research was supported by the Fundação para a Ciência e Tecnologia (FCT) through the project EXCL/QEQ-MED/0233/2012 and carried out within European COST actions TD1004. C2TN/IST authors gratefully acknowledge the FCT support through the UID/Multi/04349/2013 project. Elisabete Ribeiro acknowledges the FCT research grant.

## Abbreviations

BCMs	block copolymer micelles
DTX	docetaxel
DLS	dynamic light scattering
$D_h$	relative hydrodynamic diameter
TEM	transmission electron microscopy
LC	Drug Loading Content
LE	DTX loading efficiency
PBS	phosphate buffer (without specifications: 0.01 M pH 7.4)
DMEM	cell culture medium (Dulbecco's modified Eagle's medium)

## References

- [1] C. Allen, D. Maysinger, A. Eisenberg, Nano-engineering block copolymer aggregates for drug delivery, *Colloids Surf. B Biointerfaces* 16 (1-4) (1999) 3-27.
- [2] S.C. Baetke, T. Lammers, F. Kiessling, Applications of nanoparticles for diagnosis and therapy of cancer, *Br. J. Radiol.* 88 (1054) (2015) 20150207, <https://doi.org/10.1259/bjr.20150207>.
- [3] C.R. Bley, P. Furmanova, K. Orłowski, N. Grosse, A. Broggin-Tenzer, P.M. J. McSheehy, M. Pruschy, Microtubule stabilising agents and ionising radiation: multiple exploitable mechanisms for combined treatment, *Eur. J. Canc.* 49 (1) (2013) 245-253.
- [4] J.M. Dodewaard-de Jong van, J.M.H. Klerk, H.J. Bloemendal, Bezooijen van BPJ, M.J. Haas, R.H. Wilson, J.M. O'Sullivan, A phase I study of combined docetaxel and repeated high activity Re-186-HEDP in castration-resistant prostate cancer (CRPC) metastatic to bone (the TAXIUM trial), *Eur. J. Nucl. Med. Mol. Imag.* 38 (11) (2011) 1990-1998.
- [5] J.M. Dodewaard-de Jong van, J.M.H. Klerk, H.J. Bloemendal, D.E. Oprea-Lager, O. S. Hoekstra, H.P. van den Berg, M. Los, A. Beeker, M.A. Jonker, J.M. O'Sullivan, H. M.W. Verheul, Eertwegh van den Ajm, A randomised, phase II study of repeated rhenium-188-HEDP combined with docetaxel and prednisone versus docetaxel and prednisone alone in castration-resistant prostate cancer (CRPC) metastatic to bone; the Taxium II trial, *Eur. J. Nucl. Med. Mol. Imag.* 44 (8) (2017) 1319-1327.
- [6] M.J. Ernsting, M. Murakami, A. Roy, S.D. Li, Factors controlling the pharmacokinetics, biodistribution and intratumoral penetration of nanoparticles, *J. Contr. Release* 172 (3) (2013) 782-794.
- [7] C. Fernandes, S. Monteiro, A. Belchior, F. Marques, L. Gano, J.D.G. Correia, I. Santos, Novel Re-188 multi-functional bone-seeking compounds: synthesis, biological and radiotoxic effects in metastatic breast cancer cells, *Nucl. Med. Biol.* 43 (2) (2016) 150-157.
- [8] G. Ferro-Flores, C. Arteaga de Murphy, Pharmacokinetics and dosimetry of 188 Re-pharmaceuticals, *Adv. Drug Deliv. Rev.* 60 (12) (2008) 1389-1401.
- [9] M.R. Gill, N. Falzone, Y. Du, K.A. Vallis, Targeted radionuclide therapy in combined-modality regimens, *Lancet Oncol.* 18 (7) (2017) E414-E423.

- [10] B. Hoang, H. Lee, R.M. Reilly, C. Allen, Noninvasive monitoring of the fate of in-111-labeled block copolymer micelles by high resolution and high sensitivity MicroSPECT/CT imaging, *Mol. Pharm.* 6 (2) (2009) 581–592.
- [11] B. Hoang, R.M. Reilly, C. Allen, Block copolymer micelles target auger electron radiotherapy to the nucleus of HER2-positive breast cancer cells, *Biomacromolecules* 13 (2) (2012) 455–465.
- [12] A. Jemal, F. Bray, M.M. Center, J. Ferlay, E. Ward, D. Forman, Global cancer statistics, *Ca-a Canc. J. Clin.* 61 (2) (2011) 69–90.
- [13] R. Lange, J.M.H. de Klerk, H.J. Bloemendal, R.M. Ramakers, F.J. Beekman, M.M. L. van der Westerlaken, et al., Drug composition matters: the influence of carrier concentration on the radiochemical purity, hydroxyapatite affinity and in-vivo bone accumulation of the therapeutic radiopharmaceutical 188Rhenium-HEDP, *Nucl. Med. Biol.* 42 (2015) 465–469.
- [14] R. Lange, R. Ter Heine, T. van der Gronde, S. Selles, J. de Klerk, H. Bloemendal, et al., Applying quality by design principles to the small-scale preparation of the bone-targeting therapeutic radiopharmaceutical rhenium-188-HEDP, *Eur. J. Pharmaceut. Sci.* 30 (2016) 96–101, 90.
- [15] H. Lee, H. Fonge, B. Hoang, R.M. Reilly, C. Allen, The effects of particle size and molecular targeting on the intratumoral and subcellular distribution of polymeric nanoparticles, *Mol. Pharm.* 7 (4) (2010) 1195–1208.
- [16] H. Lee, F.Q. Zeng, M. Dunne, C. Allen, Methoxy poly(ethylene glycol)-block-poly(delta-valerolactone) copolymer micelles for formulation of hydrophobic drugs, *Biomacromolecules* 6 (6) (2005) 3119–3128.
- [17] N. Lepareur, F. Laccueille, C. Bouvry, et al., Rhenium-188 labeled radiopharmaceuticals: current clinical applications in oncology and promising perspectives, *Front. Med.* 6 (2019) 132. Published 2019 Jun 14.
- [18] C.G. Liu, Y.H. Han, R.K. Kankala, S.B. Wang, A.Z. Chen, Subcellular performance of nanoparticles in cancer therapy, *Int. J. Nanomed.* 15 (2020) 675–704.
- [19] E.B. Nejad, M.J.P. Welters, R. Arens, S.H. Burg van der, The importance of correctly timing cancer immunotherapy, *Expert Opin. Biol. Ther.* 17 (1) (2017) 87–103.
- [20] S.T. Pan, Z.L. Li, Z.X. He, J.X. Qiu, S.F. Zhou, Molecular mechanisms for tumour resistance to chemotherapy, *Clin. Exp. Pharmacol. Physiol.* 43 (8) (2016) 723–737.
- [21] E. Perez-Herrero, A. Fernandez-Medarde, Advanced targeted therapies in cancer: drug nanocarriers, the future of chemotherapy, *Eur. J. Pharm. Biopharm.* 93 (2015) 52–79.
- [22] C.A. Rabik, M.E. Dolan, Molecular mechanisms of resistance and toxicity associated with platinating agents, *Canc. Treat. Rev.* 33 (1) (2007) 9–23.
- [23] E. Ribeiro, I. Alho, F. Marques, L. Gano, I. Correia, J.D.G. Correia, S. Casimiro, L. Costa, I. Santos, C. Fernandes, Radiolabeled block copolymer micelles for image-guided drug delivery, *Int. J. Pharm.* 515 (1–2) (2016) 692–701.
- [24] T.Y. Seiwert, J.K. Salama, E.E. Vokes, The concurrent chemoradiation paradigm - general principles, *Nat. Clin. Pract. Oncol.* 4 (2) (2007) 86–100.
- [25] J.J. Shi, P.W. Kantoff, R. Wooster, O.C. Farokhzad, Cancer nanomedicine: progress, challenges and opportunities, *Nat. Rev. Canc.* 17 (1) (2017) 20–37.
- [26] R.L. Siegel, K.D. Miller, A. Jemal, Cancer statistics, *Ca - Cancer J. Clin.* 66 (2016) 7–30.
- [27] V.P. Torchilin, Micellar nanocarriers: pharmaceutical perspectives, *Pharmaceut. Res.* 24 (1) (2007) 1–16.
- [28] L.A. Torre, R.L. Siegel, E.M. Ward, A. Jemal, Global cancer incidence and mortality rates and trends-an update, *Cancer Epidemiol. Biomark. Prev.* 25 (1) (2016) 16–27.
- [29] F.Q. Zeng, H. Lee, C. Allen, Epidermal growth factor-conjugated poly(ethylene glycol)-block-poly(delta-valerolactone) copolymer micelles for targeted delivery of chemotherapeutics, *Bioconjugate Chem.* 17 (2) (2006) 399–409.